

High-Impedance Electromagnetic Surfaces with Forbidden Bands at Radio and Microwave Frequencies

D. Sievenpiper*^a, L. Zhang, R. Broas, E. Yablonovitch

Electrical Engineering Department
University of California, Los Angeles

^a Now at HRL Laboratories, Malibu, CA

ABSTRACT

A new type of metallic electromagnetic structure has been developed that is characterized by having high surface impedance. The geometry is analogous to a corrugated metal surface in which the corrugations have been folded up into lumped circuit elements, and distributed in a 2-D lattice. Although it is made of continuous metal, and conducts DC currents, it does not conduct AC currents within a forbidden frequency band. Unlike normal conductors, this new surface does not support propagating surface waves. Furthermore, image currents induced in the surface are not phase reversed as they are on a flat metal surface.

Keywords: High-impedance surface, antenna ground plane, leaky wave, photonic bandgap

1. INTRODUCTION

A flat metal sheet is used in many antennas as a reflector, or ground plane¹. The presence of a ground plane redirects half of the radiation into the opposite direction, improving the antenna gain by 3dB, and partially shielding objects on the other side. If the antenna is too close to the conductive surface, the image currents cancel the currents in the antenna, resulting in poor radiation efficiency. This problem is often addressed by including a one-quarter wavelength space between the radiating element and the ground plane, but such a structure then requires a minimum thickness of $\lambda/4$.

Another property of metals is that they support surface waves^{2,3}. These are propagating electromagnetic waves that are bound to the interface between metal and free space. They are called surface plasmons at optical frequencies⁴, but at microwave frequencies, they are nothing more than the normal currents that occur on any electric conductor. If the metal surface is smooth and flat, the surface waves will not couple to external plane waves. However, they will radiate vertically if scattered by bends, discontinuities, or surface texture. An antenna will excite surface waves that radiate from ground plane edges. The result is a kind of multipath interference or "speckle", which can be seen as ripples in the radiation pattern. Moreover, if multiple antennas share the same ground plane, surface currents can cause unwanted mutual coupling.

2. TEXTURED SURFACES

By incorporating a special texture on a conducting surface, it is possible to alter its radio-frequency electromagnetic properties^{5,6}. In the limit where the period of the surface texture is much smaller than the wavelength, the structure can be described using an effective medium model, and its qualities can be summarized into a single parameter, the surface impedance. A smooth conducting sheet has low surface impedance, but with a specially designed geometry, a textured surface can have high

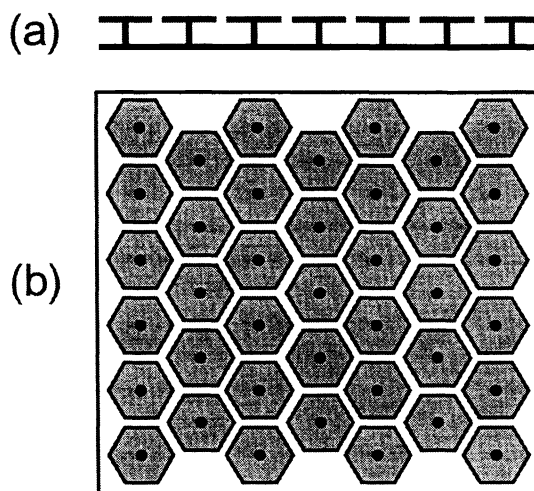


Figure 1. (a) Cross-section view and (b) top view of a high-impedance surface. The structure consists a two-dimensional array of metal protrusions connected to a solid metal ground plane. It is fabricated using printed circuit board technology, with plated metal vias connecting patches on the top surface to the ground plane on the bottom surface.

surface impedance. An example of a high-impedance surface, shown in Figure 1, consists of an array of metal protrusions on a flat metal sheet. The protrusions can be visualized as mushrooms or thumbtacks, arranged in a two-dimensional lattice on the metal surface.

If the protrusions are small compared to the operating wavelength, their electromagnetic properties can be described using lumped circuit elements – capacitors and inductors. They behave as a network of parallel resonant LC circuits, which act as a two-dimensional electric filter to block the propagation of currents along the sheet. In the frequency range where the surface impedance is very high, the tangential magnetic field is small, even with a large electric field along the surface. Such a structure is sometimes described as an artificial “magnetic conductor”.

The concept of suppressing surface waves on metals is not new. It has been done at optical frequencies using a metal sheet covered with small bumps^{7,8}. On this structure, surface waves scatter from the rows of bumps, and the resulting interference prevents them from propagating, resulting in a two-dimensional electromagnetic band gap. Our high-impedance surface can be considered as an extension of this “bumpy surface”, in which the band gap has been lowered in frequency by capacitive loading.

A related structure, the corrugated surface⁹⁻¹⁷, consists of a slab of metal into which a series of quarter-wavelength resonant slots have been cut, effectively forming a surface of high impedance at the resonance frequency of the slots. The new surface described in this paper is an abstraction of the corrugated surface, in which the corrugations have been folded up into lumped circuit elements, and distributed in a two-dimensional lattice. The surface impedance is modeled using as a parallel resonant circuit, which can be tuned to exhibit high impedance over a predetermined frequency band.

Periodic two or three-dimensional structures that prevent the propagation of electromagnetic waves are often known as photonic crystals¹⁸⁻²⁰. The high-impedance surface can be considered as a kind of two-dimensional photonic crystal that prevents the propagation of radio-frequency surface currents within the band gap. The novelty of the present work is the application of an array of lumped circuit elements to produce a thin, two-dimensional structure that must generally be described by band structure concepts²¹, even though the thickness and periodicity are both much smaller than the operating wavelength.

3. EFFECTIVE SURFACE IMPEDANCE MODEL

Surface waves can occur on the interface between two dissimilar materials, such as metal and free space. They are bound to the interface, and decay exponentially into the surrounding materials. At radio frequencies, the fields associated with these waves can extend thousands of wavelengths into the surrounding space. They are often best described as surface currents, and can be modeled from the viewpoint of an effective surface impedance^{2,3}.

Some of the properties of the high-impedance surface can be explained using an effective surface impedance model. The surface is assigned an impedance equal to that of a parallel resonant LC circuit, derived by geometry. The use of lumped parameters to describe electromagnetic structures is valid as long as the wavelength is much longer than the size of the individual features. This short wave vector range is also the regime of effective medium theory. The effective surface impedance model can predict the reflection properties and some features of the surface wave band structure, but not the band gap itself, which by definition must extend to large wave vectors.

3.1. Surface waves on impedance surfaces

Assume a surface in the YZ plane with impedance Z_s . A surface wave propagates in the +Z direction, with fields decaying in the +X direction. The geometry of the problem is shown in Figure 2. For TM surface waves, $H_x = H_z = E_y = 0$. Assume that the fields diminish in the +X direction with decay constant α , and travel along the +Z direction with propagation constant k . Start with the Z component of the electric field, given below.

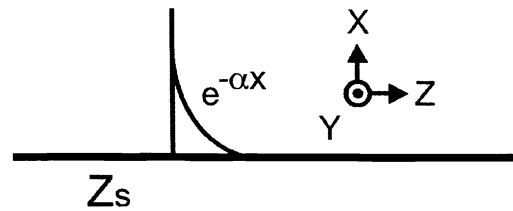


Figure 2. Geometry used for calculating surface impedance. A surface lies in the Y-Z plane, and has surface impedance, Z_s . A surface wave propagates along the surface in the +Z direction, and decays exponentially in the +X direction.

$$E_z = Ce^{-jkz-\alpha x} \quad (1)$$

H_y can be derived from the Ampere's law.

$$H_y = \frac{-j\omega\epsilon}{\alpha} Ce^{-jkz-\alpha x} \quad (2)$$

The surface impedance in this coordinate system is equal to the following expression.

$$Z_s = \frac{E_z}{H_y} \quad (2)$$

Inserting (1) and (2) into (3) gives the required surface impedance for TM surface waves.

$$Z_s(\text{TM}) = \frac{j\alpha}{\omega\epsilon} \quad (3)$$

It is clear that TM waves only occur on a surface with positive reactance – an inductive surface impedance. Using similar reasoning, we can obtain the surface impedance for TE waves, given below.

$$Z_s(\text{TE}) = \frac{-j\omega\mu}{\alpha} \quad (4)$$

Thus, a negative reactance – a capacitive surface impedance, is necessary to support TE surface waves.

3.2. Impedance of the textured surface

As the structure illustrated in Figure 3 interacts with electromagnetic waves, currents are induced in the top metal plates. A voltage applied parallel to the top surface causes charges to build up on the ends of the plates, which can be described as a capacitance. As the charges slosh back and forth, they flow around a long path through the vias and the bottom plate. Associated with these currents is a magnetic field, and thus an inductance.

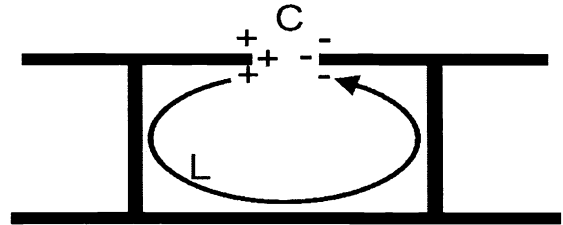


Figure 3. Origin of the capacitance and inductance in the effective surface impedance model. The proximity of the metal plates provides capacitance, while the thickness of the structure determines the inductance.

We assign to the surface a sheet impedance equal to the impedance of a parallel resonant circuit, consisting of the sheet capacitance and the sheet inductance.

$$Z = \frac{j\omega L}{1 - \omega^2 LC} \quad (5)$$

The surface is inductive at low frequencies, and capacitive at high frequencies. The impedance is very high near the resonance frequency, ω_0 .

$$\omega_0 = \frac{1}{\sqrt{LC}} \quad (6)$$

We associate the high impedance with a forbidden frequency band gap.

3.3. Surface wave band structure in the effective impedance model

We can determine the dispersion relation for surface waves in the context of the effective surface impedance model. The wave vector, k , is related to the spatial decay constant, α , and the frequency, ω , by the following expression.

$$k^2 = \mu_0 \epsilon_0 \omega^2 + \alpha^2 \quad (7)$$

For TM waves we can combine (3) with (7) to find the following expression for k as a function of ω , in which $\eta = \sqrt{\mu_0/\epsilon_0}$ is the impedance of free space, and $c = 1/\sqrt{\mu_0\epsilon_0}$ is the speed of light in vacuum.

$$k_{TM} = \frac{\omega}{c} \sqrt{1 - \frac{Z_s^2}{\eta^2}} \quad (8)$$

We can find a similar expression for TE waves by combining (4) with (7).

$$k_{TE} = \frac{\omega}{c} \sqrt{1 - \frac{\eta^2}{Z_s^2}} \quad (9)$$

By inserting (5) into (8) and (9), we can plot the dispersion diagram for surface waves, in the context of the effective surface impedance model. Depending on geometry, typical values for the sheet capacitance and sheet inductance of a two-layer structure are about 0.05 pF-square, and 2 nH/square, respectively. The complete dispersion diagram is shown in Figure 4, calculated using the effective medium model, for a structure with these parameters.

Below resonance, TM surface waves are supported. At low frequencies, they lie very near the light line, and the fields extend many wavelengths beyond the surface, as they do on a flat metal surface. Near the resonant frequency, the surface waves are tightly bound to the sheet, and have a very low group velocity, as seen by the fact that the dispersion curve is bent over, away from the light line. In the effective surface impedance limit, there is no Brillouin zone boundary, and the TM dispersion curve approaches the resonance frequency asymptotically. Thus, this approximation fails to predict the bandgap.

Above the resonance frequency, the surface is capacitive, and TE waves are supported. The lower end of the dispersion curve is close to the light line, and the waves are weakly bound to the surface, extending far into the surrounding space. As the frequency is increased, the curve bends away from the light line, and the waves are more tightly bound to the surface. The slope of the dispersion curve indicates that the waves feel an effective index of refraction that is greater than unity. This is because a significant portion of the electric field is concentrated in the capacitors. The effective dielectric constant of a material is enhanced if it is permeated with capacitor-like structures.

The TE waves that lie to the left of the light line exist as leaky waves that are damped by radiation. Radiation occurs from surfaces with a real impedance, so the leaky modes to the left of the light line are right at the resonance frequency. The radiation from these leaky TE modes can be modeled as a resistor in parallel with the high-impedance surface, which blurs the resonance frequency, radiation occurs within a finite bandwidth. The damping resistance is taken as the impedance of free space, projected onto the surface according to the angle of radiation. Small wave vectors represent radiation perpendicular to the surface, while wave vectors

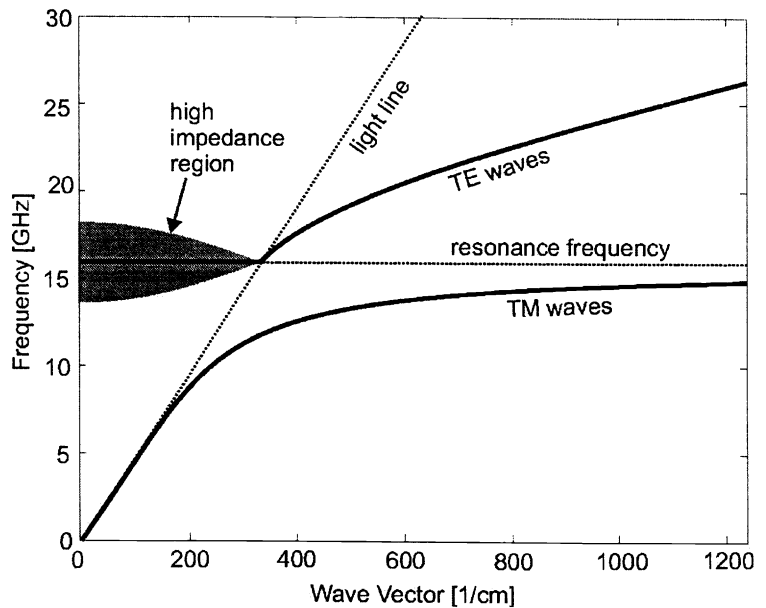


Figure 4. Surface wave dispersion diagram generated using the effective surface impedance model. Below resonance, the surface is inductive, and supports TM waves. Above resonance, the surface is capacitive, and supports TE waves. The modes that lie to the left of the light line exist as leaky modes and are damped by radiation. The effective surface impedance approximation fails to predict a band gap, but instead predicts a high-impedance region characterized by radiation damping.

near the light line represent radiation at grazing angles. The high-impedance, radiative region is shown as a shaded area, representing the blurring of the leaky waves by radiation damping. Thus, in place of a band gap, the effective surface impedance model predicts a frequency band of strong radiation damping.

3.4. Reflection phase of a high-impedance surface

The surface impedance determines the boundary condition at the surface for the standing wave formed by incident and reflected waves. If the surface has low impedance, such as in the case of a good conductor, the ratio of electric field to magnetic field is small. The electric field has a node at the surface, and the magnetic field has an antinode. Conversely, for a high-impedance surface, the electric field has an antinode at the surface, while the magnetic field has a node. Another term for such a surface is an artificial “magnetic conductor”.

Typical parameters for a two-layer ground plane are 2 nH/square of inductance, and 0.05 pF-square of capacitance. For these values, the reflection phase is plotted in Figure 5. At very low frequencies, the reflection phase is π , and the structure behaves like an ordinary, flat, metal surface. The reflection phase slopes downward, and eventually crosses through zero at the resonance frequency. Above the resonance frequency, the phase returns to $-\pi$. The phase falls within $\pi/2$ and $-\pi/2$ when the magnitude of the surface impedance exceeds the impedance of free space. Within this range, image currents are in-phase, rather than out-of-phase, and antenna elements may lie directly adjacent to the surface without being shorted out.

4. FINITE ELEMENT MODEL

In the effective surface impedance model described above, the properties of the surface are summarized into a single parameter, namely the surface impedance. Such a model correctly predicts the reflection phase, and some features of the surface wave bands. However, it does not predict an actual band gap. Nevertheless, we have found experimentally that a surface wave band gap does exist, and that the band gap edges occur where the reflection phase is equal to $\pm \pi/2$.

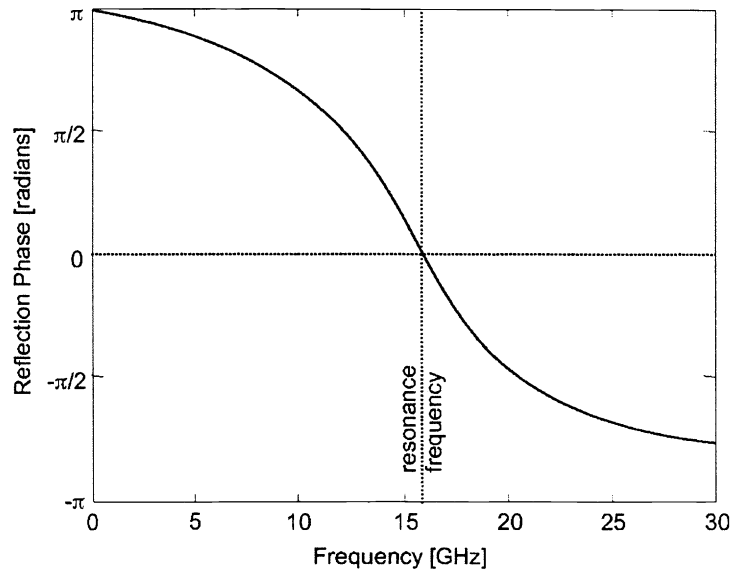


Figure 5. Reflection phase predicted by the effective surface impedance model. Far from resonance, the surface reflects with a π phase shift, just as an ordinary metal does. Near resonance, the surface reflects with a zero phase shift. In this region, image currents induced in the surface appear in-phase, rather than out-of-phase.

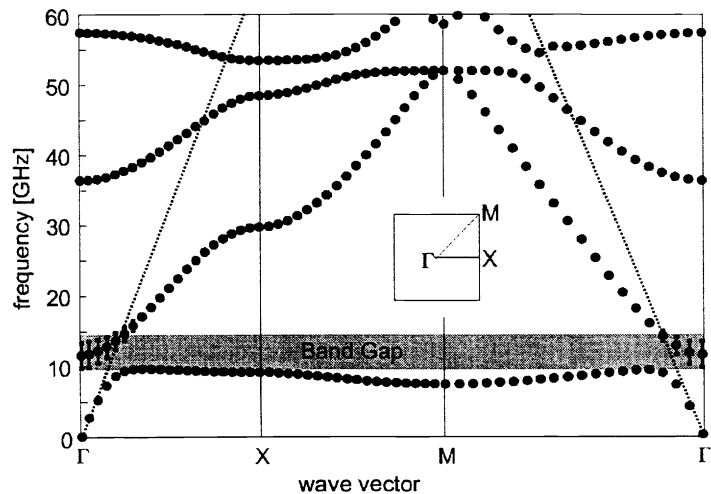


Figure 6. Dispersion diagram of a high-impedance surface with square periodicity, calculated using a finite element method. The Brillouin zone is shown as a n inset. The TM surface wave band begins at zero frequency, and levels off sharply below the resonance frequency. The TE surface wave band begins at the resonance frequency, and continues upward at less than the speed of light. The band gap extends from the top of the TM band to the point where the TE band crosses the light line. Within the band gap, TE waves exist as radiative, leaky waves. Upper bands are also seen, which do not appear in the effective surface impedance model, but are observed in the experiments.

It is necessary to obtain more accurate results using a finite element model, in which the detailed geometry of the surface texture is included explicitly. In the finite element model, the metal and dielectric regions of one unit cell are discretized on a grid. The electric field at all points on the grid can be reduced to an eigenvalue equation, which may be solved numerically. Bloch boundary conditions are used, in which the fields at one edge of the cell are related to the fields at the opposite edge by the wave vector. The calculation yields the allowed frequencies for a particular wave vector, and the procedure is repeated for each wave vector to produce the dispersion diagram. The structure analyzed by the finite element method was a two-layer, high-impedance surface with square geometry. The lattice constant was 2.4mm, the spacing between the plates was 0.15mm, and the width of the vias was 0.36mm. The volume below the square plates was filled with $\epsilon=2.2$, and the total thickness was 1.6mm.

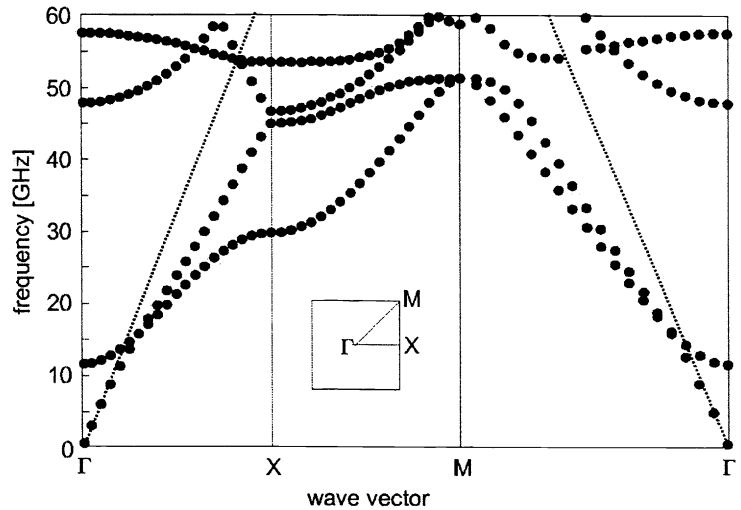


Figure 7. Finite element calculation of the surface wave band structure for a structure in which the vertical conducting vias have been removed. The band gap has vanished, and the TM band is no longer cut off. The TE band is unaffected by the absence of the vias.

The results of the finite element calculation are shown in Figure 6. The TM band follows the light line up to a certain frequency, where it suddenly becomes very flat. The TE band begins at a higher frequency, and continues upward with a slope of less than the vacuum speed of light, which is indicated on the graph by a dotted line. These results agree qualitatively with the effective medium model. The finite element method also predicts higher-frequency bands that are seen in the measurements, but do not appear in the effective medium model.

According to the finite element model, the TM band does not reach the TE band edge, but stops below it, forming a gap. The TE band slopes upward upon crossing the light line. Thus, the finite element model predicts a surface wave band gap that spans from the edge of the TM band, to the point where the TE band crosses the light line. The resonance frequency is centered in the forbidden band gap.

We have also calculated the same structure without the vertical conducting vias. The band diagram for this structure is shown in Figure 7. The TE surface waves are unaffected by the absence of the vias, and appear similar to the TE waves on the original structure. However, the TM waves are no longer terminated below the resonance frequency, as they were when the vias were present, and there is no band gap. The TM curve continues upward with a slope of slightly less than the speed of light. Therefore, the presence of the vertical connecting vias is critical for the suppression of TM surface waves, and the creation of a forbidden band.

5. MEASURING SURFACE PROPERTIES

A variety of techniques have been developed to characterize these new surfaces. The presence of surface wave modes can be measured using a pair of small probes placed near the surface, and the reflection phase can be measured using a pair of horn antennas. The measurements reveal a surface wave band gap that occurs where the reflection phase falls within $[\pi/2, -\pi/2]$. This corresponds to the region of high surface impedance.

5.1. Surface waves

Since surface waves cannot generally couple to external plane waves, specialized methods must be used to measure them. At optical frequencies, surface plasmons are often studied using a technique called prism coupling⁷. A prism is placed next to the surface, and the refractive index of the prism is used to match the wave vector of a probe beam to that of a surface wave. Another method for coupling to surface waves, which is more practical at microwave frequencies, is to use a very small probe. A point source launches all wave vectors, so a small antenna brought near the surface is capable of coupling to surface wave modes. The antenna geometry can be tailored to distinguish the surface wave polarization.

In TM surface waves, the electric field forms loops that extend vertically out of the surface. TM waves can be measured using a pair of small monopole antennas oriented normally with respect to the surface, as shown in Figure 8(a). The vertical electric field of the probe couples to the vertical electric field of the TM surface waves. In TE surface waves, the electric field is parallel to the surface, and the magnetic field forms vertical loops that arc out of

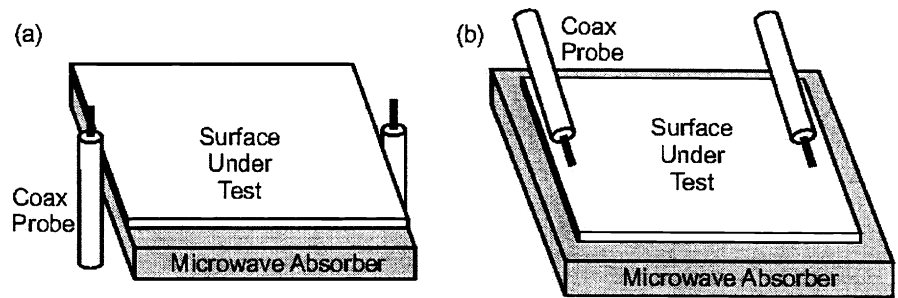


Figure 8. The presence of surface wave modes can be measured using a pair of small probes placed near the surface. The polarization of the surface waves can be distinguished by adjusting the polarization of the probes. (a) TM waves can be measured using a pair of vertical coaxial probes. (b) TE waves can be measured with a pair of horizontal probes.

the surface. They can be measured with a pair of small monopole probes oriented parallel to the sheet, as shown in Figure 8(b). The horizontal electric field of the antenna couples to the horizontal electric field of the TE waves. Since this configuration lacks the symmetry of the vertical monopole, there will be greater cross-coupling to TM waves which may complicate the measurement.

On a flat metal sheet, a TM surface wave measurement produces the results shown in Figure 9. The surface under test was a 12 cm square sheet of flat metal. The measurement represents the transmission between a pair of monopole probes oriented vertically at the edges of the metal sheet. The data has variations of 10-15 dB, but remains relatively flat over a broad spectrum. The variations are produced by multipath interference, or speckle, which occurs in coherent measurements whenever multiple signal paths are present. Multipath interference can be distinguished from other effects because it is characterized by narrow-band fading, whose details depend on the exact antenna position. The transmission drops off at low frequencies because the small probes are inefficient at exciting long wavelengths. On a flat metal surface, a TE surface wave measurement produces no significant signal, because any antenna that excites TE waves is shorted out on a conducting surface. It is only on the textured surface, with its unusual surface impedance, and tightly bound TE modes, that significant transmission signal levels can be obtained.

A typical TM surface wave measurement on a textured surface is shown in Figure 10. The size of the sheet and the measurement technique were the same as those used for the flat metal surface. The structure consisted of a triangular array of hexagonal patches, with a period of 2.54 mm and a gap between the patches of 0.15 mm. The thickness of the board was 1.55 mm, and the dielectric constant was 2.2. The transmission is strong at low frequencies, and exhibits the same multipath interference seen on the metal surface. At 11 GHz, the transmission

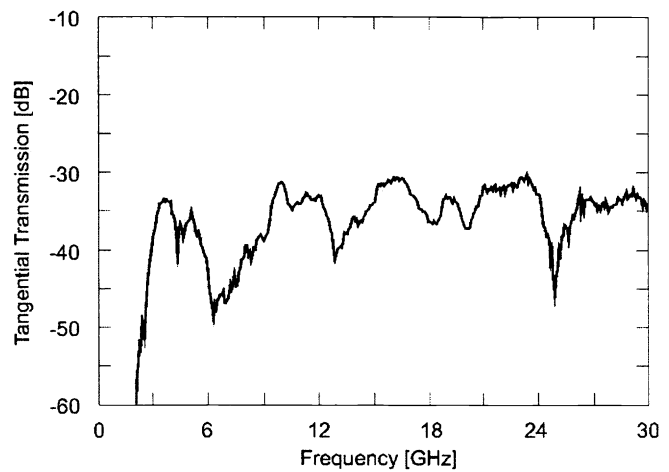


Figure 9. TM surface wave measurement of a flat metal sheet, performed using a pair of coax probes. The surface exhibits essentially flat transmission.

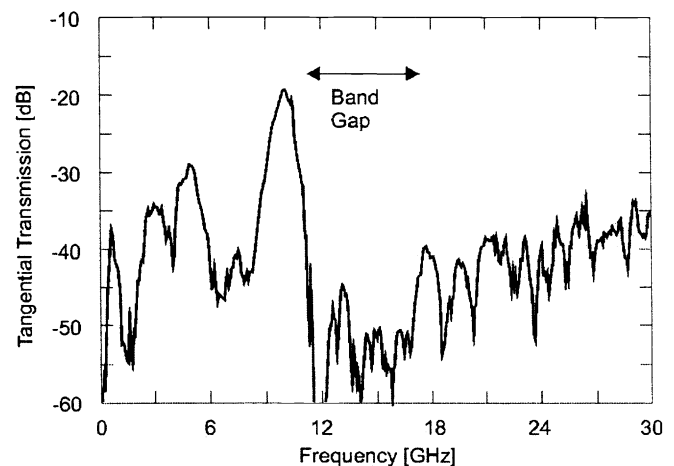


Figure 10. TM surface wave measurement of a textured, high-impedance surface. The transmission drops sharply at 11 GHz, indicating the edge of the TM band.

drops by about 30 dB, indicating the edge of the TM surface wave band. Beyond this frequency, the transmission level remains low and flat, eventually sloping upward at much higher frequencies because of weak coupling to TE surface waves. The TE band edge is not apparent in this measurement, but the region corresponding to the surface wave band gap is indicated on the graph with an arrow.

The measurement shown in Figure 11 was taken using a pair of small straight-wire coaxial probes, oriented parallel to the high-impedance surface. The transmission is weak at low frequencies, and strong at high frequencies, the reverse of the TM data. A sharp jump of 30 dB occurs at 17 GHz, indicating the TE band edge. Beyond this frequency, the transmission is flat, with only small fluctuations due to speckle. The TE probes also couple slightly to TM surface waves, so there is an additional transmission peak at 11 GHz, at the TM band edge, where the density of TM states is high. Both TM and TE probes tend to couple slightly to both surface wave polarizations. However, the cross-coupling is weaker between the TM probe and the TE surface waves because of the symmetry of the vertical monopole.

A surface wave band gap exists between the TM band edge at 11 GHz and the TE band edge at 17 GHz. Within this range, neither type of measurement produces significant transmission. Currents cannot propagate across the surface, and any currents induced in the surface radiate rapidly into free space.

5.2. Reflection phase

The reflection phase of the high-impedance surface can be measured using two microwave horn antennas, as shown in Figure 12. The measurement is done in an anechoic chamber lined with microwave absorbing foam. The two horns are placed next to each other, aimed at the surface. Two windows are cut in the chamber, one for the antennas, and one for the surface under test.

A reference measurement is taken of a surface with known reflection properties, such as a flat sheet of metal, and all subsequent measurements are divided by this reference. A factor of π is added to the phase data to account for the reference scan of the metal sheet, which is known to have a reflection phase of π .

The reflection phase of the high impedance surface is shown in Figure 13. At low frequencies, it reflects with a π phase shift, just like a flat metal surface. As the frequency is increased, the phase slopes downward, and eventually crosses through zero at the resonance frequency of the structure. At higher frequencies, the phase continues to slope downward, and eventually

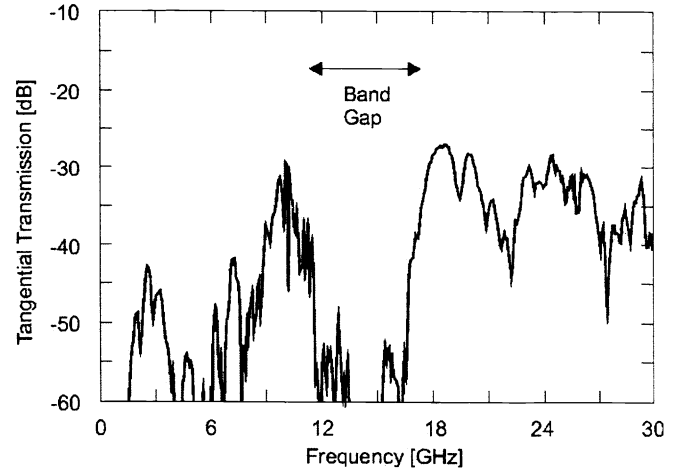


Figure 11. TE surface wave measurement of a textured, high-impedance surface. The TE band edge can be seen at 17 GHz, where the transmission suddenly increases sharply. Some cross-coupling can also be seen at the TM band edge at 11 GHz.

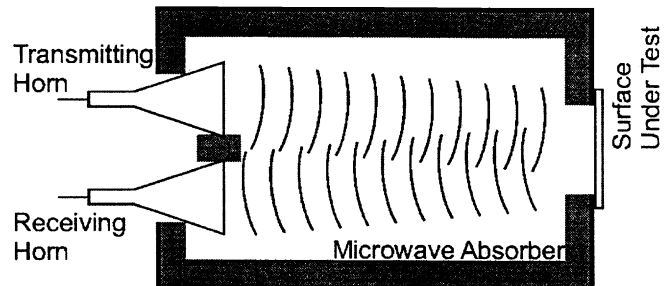


Figure 12. Measurement of the reflection phase using a pair of horn antennas and an anechoic chamber.

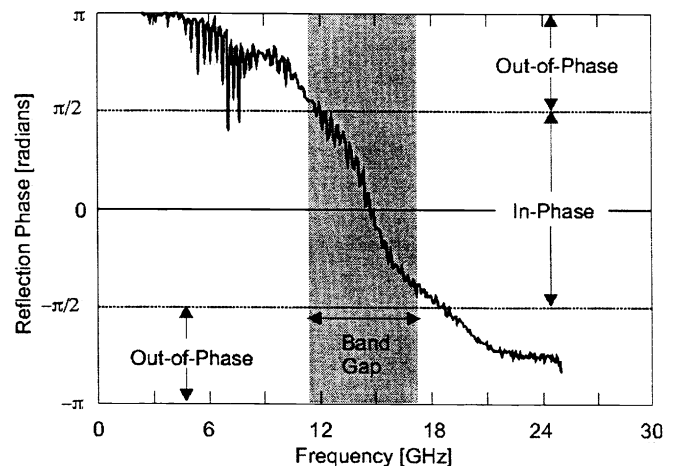


Figure 13. Reflection phase measurement of the textured, high-impedance surface. Within the band gap, image currents induced in the surface appear in-phase, rather than out-of-phase. At the resonance frequency, the surface can be considered as an artificial “magnetic conductor”.

approaches $-\pi$. Within the region between $\pi/2$ and $-\pi/2$, indicated on the graph by arrows, plane waves are reflected in-phase, rather than out-of-phase. This range also corresponds to the measured surface wave band gap, indicated on the graph by a shaded region, with the TM and TE band edges falling approximately at the points where the phase crosses through $\pi/2$ and $-\pi/2$, respectively.

6. LOW-FREQUENCY STRUCTURES

With two-layer construction shown in Figure 1, the capacitors are formed by the fringing capacitance between two metal plates lying edge-to-edge, usually separated by a few hundred microns. If the substrate has a dielectric constant between 2 and 10, and the period is a few millimeters, the capacitance is generally on the order of several tens of fF. With a thickness of a few mm, the inductance is a few nH, so the resonance frequency is on typically the order of about 10 GHz.

If the desired resonance frequency is less than about 5 GHz, the thickness can be kept within reasonable limits by using three-layer construction, in which the capacitors are formed between overlapping metal plates, as shown in Figure 14. In this geometry, parallel-plate capacitors are formed by the top two overlapping layers, and a capacitance of several pF is easily achievable. Resonance frequencies of less than 1 GHz can be produced, while maintaining the thickness and period on the order of a few mm. However, by forcing a thin structure to have a low resonance frequency, the bandwidth is also reduced.

The three-layer structure studied here had a hexagonal lattice, with a period of 6.35 mm, and an overlap area between adjacent metal plates of 6.84 mm^2 . The spacer layer between the plates had a thickness of $100 \mu\text{m}$, and a dielectric constant of 3.25. The lower, supporting board was 3.17 mm thick, with a dielectric constant of 4.

The three-layer, high-impedance surface maintains the same general properties as the two-layer structure, with TM and TE surface wave bands separated by a gap, within which there are no propagating surface wave modes. A surface wave measurement is shown in Figure 15 for transmission between two straight coaxial probes lying parallel to the surface. The frequency is low enough that the free-space wavelength is much greater than the probe length, which is only a few millimeters, so the antennas tend to couple equally well to TM and TE modes. Transmission can be seen in both the TM and TE bands, and a gap is visible between 2.2 and 2.5 GHz.

The reflection phase of the three layer structure is shown in Figure 16. The region corresponding to the surface wave band gap is designated by arrows. Inside the gap,

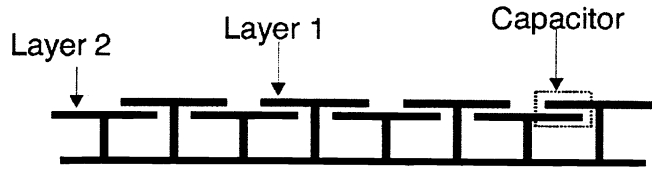


Figure 14. A lower resonance frequency is obtained for a given thickness by using capacitive loading. This can be achieved by using a three-layer geometry, in which the top two layers consist of overlapping metal plates, separated by an insulating layer.

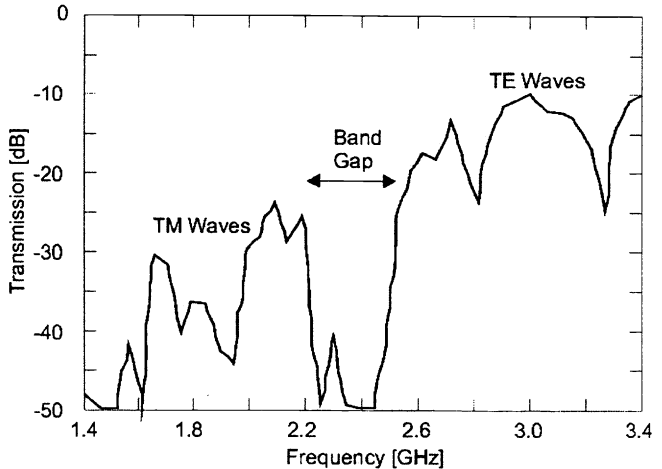


Figure 15. A surface wave transmission measurement on a three layer high-impedance surface, measured in what is usually considered TE configuration. Because the probes are so small compared to the wavelength, they couple well to both polarizations. The band gap can be seen between 2.2 and 2.5 GHz.

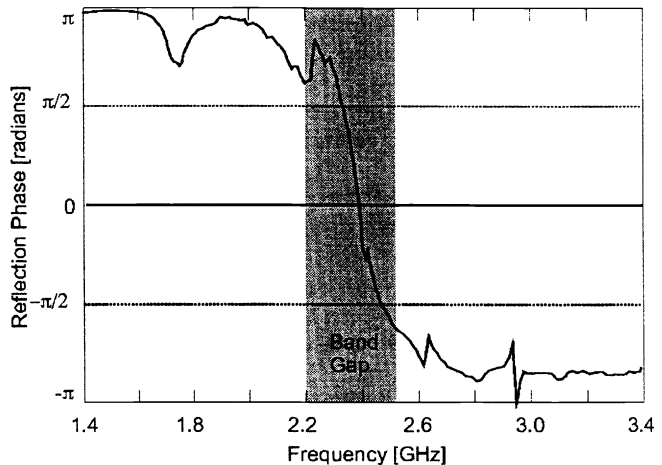


Figure 16. Reflection phase measurement of the three-layer, high-impedance surface. As was seen in the two-layer structure, the measured surface wave band gap coincides with the frequency range where the image currents are in-phase.

the reflection phase crosses through zero, and plane waves are reflected in-phase rather than out-of-phase.

Until now, we have focused primarily on frequencies near the high-impedance condition, where the TM band ends, the reflection phase crosses through zero, and the TE band begins. There are numerous other interesting electromagnetic features at higher frequencies, which could be the subject of further study. Some of these features are illustrated in Figure 17, which shows the surface wave transmission across the three-layer structure, measured over a broader frequency range.

The TM band is visible up to 2.2 GHz, where the first gap begins. The TE band begins at 2.5 GHz, and continues up to about 5.5 GHz where a second, much wider gap begins. In this second gap, there are no detectable surface waves, but the structure does not exhibit the favorable surface impedance of the first gap. It is not known whether the second gap can be useful for electromagnetic devices. The second gap is followed by an upper band, which was also seen in the finite element calculations, in Figure 6. These modes lie within the lower dielectric region between the top metal plates, and resemble the modes of a parallel plate waveguide. This band occurs at the frequency where one-half wavelength fits between the rows of vias.

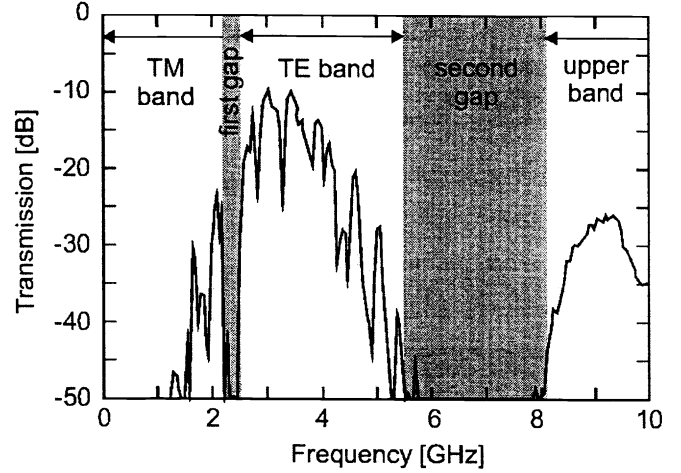


Figure 17. Broad transmission spectrum for the three-layer high-impedance surface.

7. FUNDAMENTAL LIMITATIONS

Through capacitive loading, one can produce a structure with a lower resonant frequency for a given thickness. However, this also reduces the width of the band gap, as well as the high-impedance region within which the surface currents radiate. We can estimate the frequency range over which the surface waves radiate by using a circuit model. The textured surface is modeled as an LC circuit, and the radiation into free space is modeled as a resistor with a value of $\sqrt{\mu_0/\epsilon_0}/\cos(\theta) = 377\Omega/\cos(\theta)$, where θ is the angle of the radiation with respect to the surface. The amount of power dissipated in the resistor is a measure of the radiation efficiency of the surface waves.

The maximum power dissipated in the resistor occurs at the LC resonance frequency of the ground plane, where the surface reactance crosses through infinity. It can be shown that the frequencies where the radiation drops to half of its maximum value occur when the magnitude of the surface impedance is equal to the impedance of free space. For radiation perpendicular to the surface, we have the following equation.

$$\left| \frac{j\omega L}{1 - \omega^2 LC} \right| = \eta \quad (10)$$

This can be solved for ω , to yield the equation below.

$$\omega^2 = \frac{1}{LC} + \frac{1}{2\eta^2 C^2} \pm \frac{1}{\eta C} \sqrt{\frac{1}{LC} + \frac{1}{4\eta^2 C^2}} \quad (11)$$

For typical geometries, L is usually on the order of 1 nH, and C is in the range of 0.05–10 pF. With these values, the terms involving $1/\eta^2 C^2$ are much smaller than the $1/LC$ terms, so we will eliminate them. This approximation yields the following expression for the boundaries of the high-impedance region.

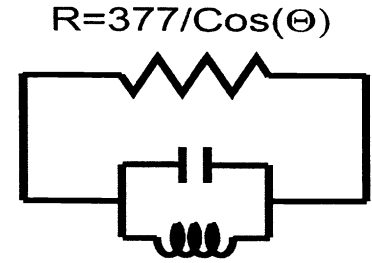


Figure 18. Equivalent circuit used to estimate the bandwidth over which the surface waves radiate. The radiation is modeled as a resistor, whose value depends on the angle of radiation.

$$\omega = \omega_0 \sqrt{1 \pm \frac{Z_0}{\eta}} \quad (12)$$

The resonance frequency is $\omega_0 = 1/\sqrt{LC}$, and $Z_0 = \sqrt{L/C}$ is the characteristic impedance of the LC circuit. With the parameters for L, C, and η given above, Z_0 is usually significantly smaller than η . Thus, the square root can be expanded in the following approximation.

$$\omega \approx \omega_0 \left(1 \pm \frac{1}{2} \frac{Z_0}{\eta} \right) \quad (13)$$

The two frequencies designated by the +/- signs delimit the range over which the TE surface waves are highly damped by radiation. The total bandwidth is roughly equal to the characteristic impedance of the surface divided by the impedance of free space.

$$\frac{\Delta\omega}{\omega_0} = \frac{Z_0}{\eta} \quad (14)$$

This is also the bandwidth over which the reflection coefficient falls between $+\pi/2$ and $-\pi/2$, and image currents are more in-phase than out-of-phase. Thus, it represents the maximum usable bandwidth of an antenna on a resonant surface of this type.

The resonance frequency is given by $\omega = 1/\sqrt{LC}$, so it can be lowered by increasing either the inductance or the capacitance. The sheet inductance, $L = \mu t$, depends on the thickness of the structure, as well as the permeability. Since low-loss, high-permeability materials do not currently exist at microwave frequencies, the inductance is fixed by the thickness. Thus, the only way to lower the resonance frequency for a given thickness is to use capacitive loading.

The relative bandwidth, $\Delta\omega/\omega$, is proportional to $\sqrt{L/C}$, so if the capacitance is increased, the bandwidth suffers. Since the thickness is related to the inductance, the more the resonance frequency is reduced for a given thickness, the more the bandwidth is diminished. It would appear that a structure has a certain “natural frequency” that depends on the thickness, and that the bandwidth is related to the ratio of the actual resonance frequency to this natural frequency. This is suggested by the equation below.

$$\frac{\Delta\omega}{\omega_0} = \frac{\omega_0}{\omega_{\text{natural}}} \quad (15)$$

This can be solved to yield the natural frequency as a function of the physical parameters of the structure.

$$\omega_{\text{natural}} = \frac{c}{\mu_r t} \quad (16)$$

In the above equation, c is the speed of light in vacuum, while μ_r and t are the relative magnetic permeability and the thickness, respectively, of the material filling the lower, inductive part of the structure, as shown in Figure 19. Since the dielectric constant does not appear in (16), the bulk of a three-layer structure can be filled with a low-dielectric material without affecting frequency or bandwidth. In the two-layer structures, in which the capacitance is determined by the fringing electric fields that extend into the lower dielectric material, the relation given in (16) is still satisfied, but the dielectric constant influences ω_{natural} .

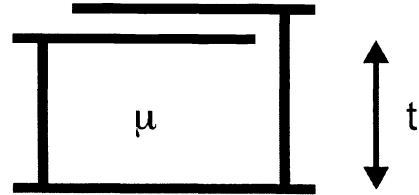


Figure 19. Cross section view of a three-layer, high-impedance surface. At microwave frequencies, where low-loss, high-permeability materials are unavailable, the bandwidth depends only on the thickness of the structure with respect to the wavelength at resonance.

8. CONCLUSION

A new type of metallic electromagnetic structure has been developed that is characterized by having high surface impedance. It is made of continuous metal, and conducts DC currents, but it does not conduct AC currents within a forbidden frequency band gap. Instead, any currents that are induced in the surface radiate efficiently into surrounding space. This new surface also reflects electromagnetic waves with no phase reversal, behaving as a kind of artificial magnetic conductor. The structure can be described using a lumped parameter circuit model, which predicts some of its electromagnetic properties.

ACKNOWLEDGEMENTS

This work was supported by Army Research Office grant DAAH04-96-1-0389, HRL Laboratories subcontract number S1-602680-1, and Office of Naval Research grant N00014-99-1-0136.

REFERENCES

1. C. Balanis, Antenna Theory, Analysis, and Design, 2nd ed., John Wiley and Sons, New York (1997)
2. S. Ramo, J. Whinnery, T. Van Duzer, Fields and Waves in Communication Electronics, 2nd ed., John Wiley and Sons, New York (1984)
3. R. Collin, Field Theory of Guided Waves, 2nd ed., IEEE Press, New York (1991)
4. H. Raether, Surface Plasmons on Smooth and Rough Surfaces and on Gratings, Springer-Verlag, New York (1988)
5. D. Sievenpiper, "High-Impedance Electromagnetic Surfaces", Ph.D. Dissertation, University of California, Los Angeles, 1999
6. D. Sievenpiper, E. Yablonovitch, "Circuit and Method for Eliminating Surface Currents on Metals", U. S. provisional patent application, serial number 60/079953, filed on March 30, 1998
7. W. Barnes, T. Priest, S. Kitson, J. Sambles, "Photonic Surfaces for Surface-Plasmon Polaritons", *Phys. Rev. B* 54, 6227 (1996)
8. S. Kitson, W. Barnes, J. Sambles, "Full Photonic Band Gap for Surface Modes in the Visible", *Phys. Rev. Lett.* 77, 2670 (1996)
9. A. Harvey, "Periodic and Guiding Structures at Microwave Frequencies", *IRE Trans.* 8, 30 (1959)
10. C. Elachi, "Waves in Active and Passive Periodic Structures: A Review", *Proc. IEEE* 64, 1666 (1976)
11. L. Brillouin, "Wave Guides for Slow Waves", *J. App. Phys.* 19, 1023 (1948)
12. W. Rotman, "A Study of Single-Surface Corrugated Guides", *Proc. IRE* 39, 952 (1951)
13. R. Elliot, "On the Theory of Corrugated Plane Surfaces", *IRE Trans. Ant. Prop.* 2, 71 (1954)
14. S. Lee, W. Jones, "Surface Waves on Two-Dimensional Corrugated Surfaces", *Radio Science* 6, 811 (1971)
15. Y.-L. Chen, Y. Lo, "Reactive Reflectors", *IEE Proc. H* 131, 263 (1984)
16. P.-S. Kildal, "Artificially Soft and Hard Surfaces in Electromagnetics", *IEEE Trans. Ant. Prop.* 38, 1537 (1990)
17. Z. Ying, P.-S. Kildal, A. Kishk, "Study of Different Realizations and Calculation Models for Soft Surfaces by Using a Vertical Monopole on a Soft Disk as a Test Bed", *IEEE Trans. Ant. Prop.* 44, 1474 (1996)
18. G. Kurizki, J. Haus, eds., Photonic Band Structures, *Journal of Modern Optics* 41, special issue (1994)
19. J. Joannopoulos, R. Meade, J. Winn, Photonic Crystals: Molding the Flow of Light, Princeton University Press, Princeton (1995)
20. C. Soukoulis, ed., Photonic Band Gap Materials, Proceedings of the NATO ASI on Photonic Band Gap Materials, Elounda, Crete, Greece, June 18-30, 1995, Kluwer Academic Publishers, The Netherlands (1996)
21. L. Brillouin, Wave Propagation in Periodic Structures; Electric Filters and Crystal Lattices, 2nd ed., Dover Publications, New York (1953)